

Supplementary Information

S1 Experimental details

The ZnO films were deposited using RF magnetron sputtering. High purity (99%) ZnO sputtering target (Vin Karola Instruments) was used in the process. The sputtering process was started after the chamber was pumped down to 2×10^{-5} torr. Al₂O₃ substrates were used after being adequately cleaned using acetone, isopropanol and distilled water successively, and dried using a high pressure nitrogen gun. The substrates were kept at room during the sputtering process. RF sputtering power of 160 W was used throughout the deposition process. The sputtering process was carried out under an atmosphere of 100% Argon (Ar). A sputtering time of 60 mins resulted in $\sim 1 \mu\text{m}$ ZnO layer. Adhesive conductive silver (Ag) paste (42469, Alfa Aesar) was used to make electrical contacts between the copper tape electrodes and the ZnO samples. Nitrocellulose [C₆H₈(NO₂)₂O₅] was used as the fuel due to its large enthalpy of reaction. Nitrocellulose was prepared by dissolving millipore nitrocellulose membranes (N8645, Sigma Aldrich) in acetonitrile (15 g L⁻¹). This solution was drop-cast onto the ZnO film and dried at 50° C. The acetonitrile evaporated, leaving a layer of adhesive nitrocellulose coating. Sodium azide (NaN₃) (14314, Alfa Aesar) in aqueous solution (50 mg mL⁻¹) was then added on top of the nitrocellulose layer using a pipette to serve as a primary igniter. The Raman spectra were recorded with a system incorporating an Ocean Optics QE 6500 spectrometer, and a 532 nm 40 mW laser as the excitation source.

XRD was carried out using a Bruker D8 DISCOVER microdiffractometer fitted with a GADDS (General Area Detector Diffraction System). Data was collected at room temperature using CuK α radiation ($\lambda = 1.54178 \text{ \AA}$) with a potential of 40 kV and a current of 20 mA, and filtered with a graphite monochromator in the parallel mode (175 mm collimator with 0.5 mm pinholes).

Scanning electron microscopy (SEM) was conducted using the FEI Nova Nano SEM to investigate the structure of the ZnO films.

S2 Calculation of specific power

In order to obtain the specific power, the masses of the fuel (nitrocellulose & sodium azide) and thermoelectric films were considered. The relationship between mass, density and volume was used for calculating the mass of the ZnO films as: $m = \rho \times V$, where, m is the mass in grams (g), ρ is the density in g cm⁻³ and V is the volume in cm³.

$\rho = 5.6 \text{ g.cm}^{-3}$ for ZnO and V depends on the dimensions of the sample and is calculated using the formula, $V = l \times w \times h$ where l is the length, w is the width and h is the thickness of the thermoelectric film in cm, respectively. For fuels, nitrocellulose and NaN₃ in our case, we knew the concentration of the two in their respective solutions. As mentioned in the main manuscript, 15 g L⁻¹ nitrocellulose and 20 g L⁻¹ NaN₃ were used by drop casting. Hence, we know the amount of solution for each fuel and

therefore the corresponding mass for each sample, depending on the volume of the liquid placed on the thermoelectric films. The sum of the masses of the thermoelectric film and the fuels gives the total mass of the materials used. The corresponding power from the sample is obtained using the equation: $P = \frac{V}{R}$ in which P is the peak power in watts, V is the peak output voltage in volts and R the resistance in Ω .

The output power is then scaled to per kg of the materials to obtain the specific power of the sample in kW kg⁻¹.

S3 Voltage, current, power and specific power data obtained for all thermopower devices

Figure S1a below shows the voltage and current outputs obtained from the fuel/ZnO/Al₂O₃ thermopower devices. It can be seen that peak voltage and current of approximately 500 mV and 2 mA, respectively, were obtained. The peak power and specific power output were approximately 1 mW and 500 W/kg, respectively, and are shown in Figure S1b.

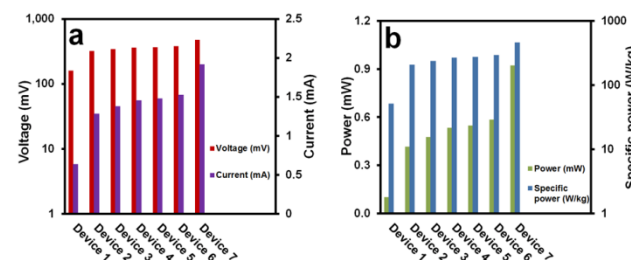


Fig S1 Outputs a) voltage and current b) power and specific power obtained from the fuel/ZnO/Al₂O₃ thermopower devices.

S4 Measurement of Seebeck coefficient

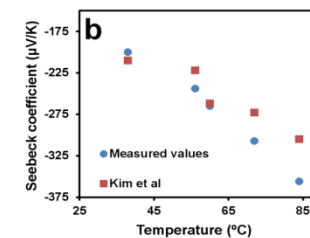
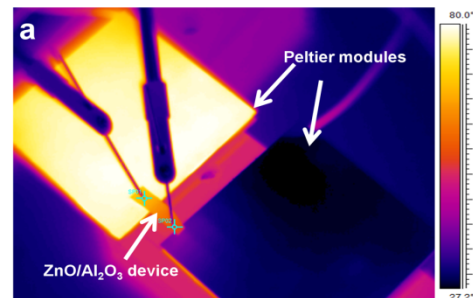


Fig S2 a) Measurement set up used to calculate the Seebeck coefficient. The above image has been obtained using an infrared camera b) Measured and literature values of the Seebeck coefficient at different temperatures.¹⁵

The experimental set up to measure the Seebeck coefficient is shown in Figure S2a. The temperature difference was attained using two Peltier modules. The sample was placed such that one edge rested on the hot side of one Peltier module while the other edge rested on the cold side of the other module. Micromanipulator probes were then used to measure the voltage generated as a result of the temperature difference. An infrared camera (FLIR Systems, ThermoVision A320, Sweden) interfaced with ThermaCAM Researcher software was used to accurately measure the temperature difference at the two ends of the sample. Measurements were made up to a temperature of 85 °C. Figure S2b shows a comparison of the measured Seebeck coefficient at different temperatures with the literature values. The Seebeck coefficient obtained at 85 °C is approximately $-360 \mu\text{V.K}^{-1}$. It shows that the measurement values are comparable to those obtained by Kim *et al.*¹⁸

S5 Detailed analysis of the Raman spectroscopy results

In a wurtzite ZnO crystal there are 4 atoms per unit cell and a total of 12 phonon modes. These include one longitudinal-acoustic (LA), two transverse-acoustic (TA), three longitudinal-optical (LO) and six transverse-optical (TO) branches. The A_1 and E_1 branches are both Raman and infrared active while the two non-polar E_2 branches are Raman active only.

Figure 3(b), 1 illustrates the Raman spectra of the as-grown ZnO structure. The peaks observed at around 436 cm^{-1} , 576 cm^{-1} correspond to the E_2 (high) and the A_1 (LO) modes respectively. For lattice vibrations with A_1 symmetries the atoms move parallel to the c axis while the high frequency E_2 mode involves the vibrations of the oxygen atoms.

If the incident light is normal to the surface and only, A_1 (LO) and E_2 modes are observed, it implies that the film is highly oriented. The E_2 (high) is a characteristic mode of the ZnO hexagonal wurtzite type lattice.²⁸ Therefore, the Raman results prove that the fabricated ZnO films are highly oriented.

The Raman peaks after the deposition of nitrocellulose Figure 3(b), 2 shows the presence of strong C–H bonds as well as weak NO₂ bonds.³⁸ After the thermopower wave propagation the C–H bonds disappear while carbon peaks appear on the Raman spectra Figure 3(b), 3. The exothermic reaction causes the C–H bonds to decompose while carbon is left behind as the residual product.

S6 Atomic Force Microscopy

Atomic force microscopy (AFM) was carried out on the ZnO films using a AFM-Bruker D3100 in order to assess their surface roughness. A higher porosity is important for an increased thermal conduction between the fuel layer and the ZnO surface thereby resulting in a more sustained reaction propagation. Figures S3a & S3b show the 2D and 3D profiles of the ZnO film surface sample, respectively. The ZnO films exhibit a root mean squared roughness of $\sim 250 \text{ nm}$ indicating strong porous nature of the films.

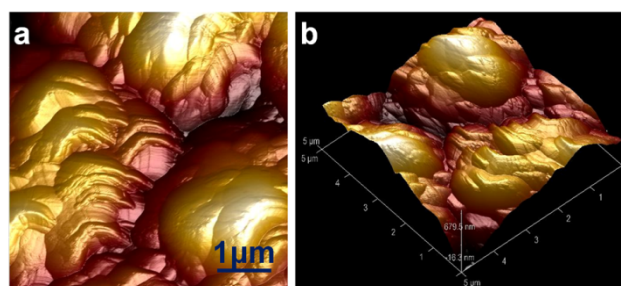


Fig S3 samples of AFM images: a) 2D image of the ZnO film surface b) 3D profile of the ZnO film surface

60

S7 Thermal conduction behaviour

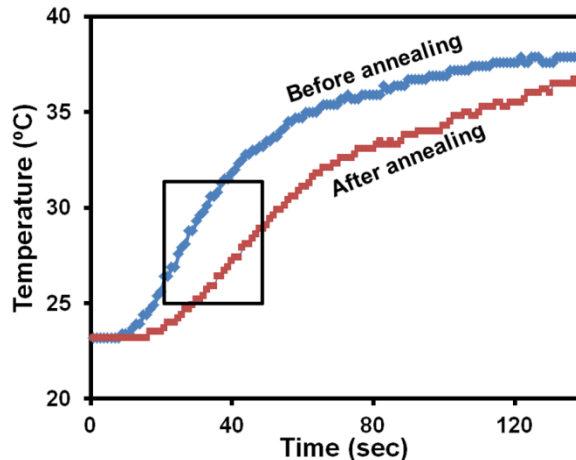


Fig S4: Change in thermal conduction of the ZnO films before and after annealing at 300 °C.

65

To emulate the effect of surface heating on ZnO film during the thermopower propagation reaction, a ZnO/Al₂O₃ sample was annealed at 300 °C for 1 min in a vacuum furnace. Its thermal conduction behaviour was compared with the non-annealed sample. Additionally, its crystal structure was also examined after annealing.

In order to make the thermal conductivity comparison, one end of the sample with ZnO film was rested on a heater at 40 °C and the temperature was recorded at the opposite end. Figure S4 shows the results after 150 seconds of measurements. The slope of the rise in temperature with time highlights the rate at which heat is transferred from one end to the other. The slope of the temperature rise was calculated to be $0.28 \text{ }^{\circ}\text{C} / \text{s}$ before annealing while it decreased slightly to $0.22 \text{ }^{\circ}\text{C}/\text{s}$ after annealing. This directly translates into less than 25% decrease in thermal conductivity. As a result, the thermal conductivity shows a small reduction in value after annealing.

85

S8 Characterization after annealing

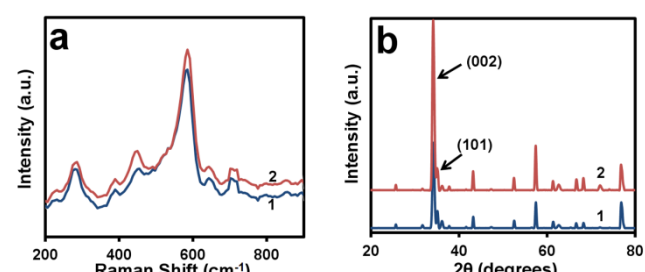


Fig S5: (a) Raman peaks of ZnO films 1. before and 2. after thermal annealing at 300 °C, (b) XRD pattern of 1.ZnO film before and 2. after annealing

Figures S5a and S5b show the Raman spectra and XRD patterns of the ZnO films before and after annealing, respectively. The XRD shows that the relative intensity of the dominant (002) to the (101) peak increases slightly (approximately 7%) after annealing.^{4S} This indicates the *c* axis directional orientation of the ZnO enhanced marginally after annealing. Additionally, the Raman spectra also does not identify any significant change as a result of annealing.

15

References for the Supplementary

- [1S] K. H. Kim, S. H. Shim, K. B. Shim, K. Niihara and J. Hojo, *J. the Amer. Ceram. Soc.*, 2005, **88**, 628.
[2S] U. Ozgur, Y. I. Alivov, C. Liu, A. Teke, M. A. Reshchikov, S. Dogan, V. Avrutin, S. J. Cho and H. Morkoc, *J. App. Phys.*, 2005, **98**, Art. No. 041301.
[3S] D. S. Moore and S. D. McGrane, *J. Mol. Str.*, 2003, **661**, 561.
[4S] J. Kim, M. Kim, J. Yu and K. Park, *Curr.Appl. Phys.*, 2010, **10**, 495.